THE JOURNAL OF PHYSICAL CHEMISTRY C
A JOURNAL OF THE AMERICAN CHEMICAL SOCIETY

pubs.acs.org/JPCC

Article

CO_2 Activation on Ceria: Polarization-Resolved Infrared Identification of Surface Carbonates on CeO_2(110)

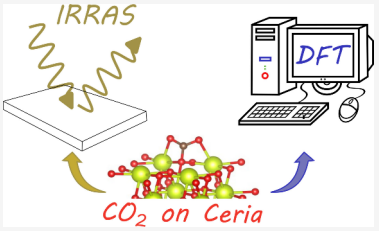
Johannes Döhn,[#] Chengwu Yang,[#] Axel Groß,[*] and Christof Wöll[*]

Cite This: https://doi.org/10.1021/acs.jpcc.6c06381

Read Online

ACCESS | Metrics & More | Article Recommendations | Supporting Information

ABSTRACT: Understanding CO_2 activation on ceria is central to elucidating elementary steps in catalytic CO_2 conversion, yet direct vibrational identification of carbonate species on well-defined ceria single crystals has remained elusive. Here, we use polarization-resolved infrared reflection−absorption spectroscopy to identify surface carbonates formed upon CO_2 adsorption on oxidized CeO_2(110), with surface quality confirmed using CO as a probe molecule and X-ray photoelectron spectroscopy. Alongside molecularly physisorbed CO_2, we observe bands at 1510 and 1280 cm^{-1} that we assign to a monodentate carbonate on the stoichiometric surface; their distinct polarization dependence matches the adsorption geometry predicted by density functional theory, giving direct experimental validation of the proposed structure. Additional bands at 1570 and 1610 cm^{-1}, absent from the ideal-surface picture, are tentatively assigned to carbonates at defective sites such as step edges or oxygen vacancies. By establishing definitive, structurally validated vibrational fingerprints for CO_2 activation on a single-crystal ceria surface, this work provides an essential molecular-level reference for interpreting infrared spectra of ceria-based powder catalysts.



INTRODUCTION

The catalytic hydrogenation of CO_2 is widely recognized as a key process for the sustainable production of fuels and chemicals, offering a route to close the anthropogenic carbon cycle and mitigate greenhouse gas emissions.[1−4] A molecular-level understanding of CO_2 activation and transformation at solid surfaces is therefore of central importance for the rational design of improved catalysts. In this context, vibrational spectroscopy—most notably infrared (IR) spectroscopy—has proven to be an indispensable tool for unraveling fundamental aspects of surface chemistry, as it provides direct access to the structure, bonding, and dynamics of adsorbed species. Furthermore, DRIFTS (diffuse reflectance infrared Fourier transform spectroscopy) can be applied to powder samples at ambient pressure,[5] allowing for operando studies.

Despite the extensive body of work on cerium dioxide as a model and technologically relevant oxide, the interaction of CO_2 with well-defined ceria surfaces remains insufficiently understood. While the formation of carbonate species on single crystal ZnO(10−10) surfaces has been studied using IRRAS (infrared reflection−absorption spectroscopy),[6] no experimental infrared spectroscopic studies on carbonate species resulting from CO_2 exposure at ceria single-crystal surfaces have been reported to date. In an earlier NEXAFS (near edge X-ray absorption fine structure) and XPS (X-ray photoelectron spectroscopy) study, exposure of CeO_2(110) surfaces to CO_2 was reported to lead to the formation of two species, a physisorbed and chemisorbed species.[7] The latter was identified as carbonate. No IR data were reported in this study, which hampers the assignment of peaks observed when exposing ceria powders to CO_2.

On the theoretical side, vibrational frequencies of carbonate species on ceria have been reported for the CeO_2(111) surface,[8,9] whereas for the more reactive CeO_2(110) facet only adsorption geometries and binding energies have been addressed.[10,11] Experimental investigations are largely limited to DRIFTS studies on powder samples.[12] However, owing to the irregular morphology and heterogeneous nature of oxide powders, these measurements do not permit an unambiguous assignment of vibrational bands to specific adsorption configurations or surface sites. For a reliable assignment of species formed after exposing powders to CO_2, reference data for well-defined single-crystal surfaces are urgently required.

Under ultrahigh vacuum (UHV) conditions, it has been shown experimentally using IRRAS that on the thermodynamically most stable CeO_2(111) surface, CO_2 adsorbs exclusively in a linear, physisorbed configuration at low temperature and pressure (80 K, pressure <1 × 10^{-6} mbar).[13] Carbonate species were predicted by theory[8] to exist on this close-packed, energetically most favorable surface of ceria, but experimentally such a chemisorbed species has not yet been observed on CeO_2(111). More open and thus more reactive surface terminations must therefore be considered in order to experimentally access chemically activated CO_2 species on

Received: September 17, 2026
Revised: October 16, 2026
Accepted: October 19, 2026

Downloaded from pubs.acs.org/jpccck/article-pdf/doi/10.1021/acs.jpcc.6c06381/6906427/acs.jpcc.6c06381.pdf by UNIV ULM user on 05 November 2026

© XXXX American Chemical Society

this oxide. Among the low-index ceria surfaces, $CeO_2(110)$ is of particular interest, since the third low-index surface, $CeO_2(100)$, undergoes reconstruction and is therefore less suitable as a well-defined model system for determining the vibrational frequencies of activated CO_2 on ceria. Previous theoretical work by Saniz and co-workers[10] identified the formation of a carbonate species on $CeO_2(110)$ and provided detailed structural insight; however, vibrational frequencies for these species were not reported, precluding direct comparison with experiment and assignment of the peaks observed for CO_2-exposed ceria powders.

In the present study, we employ polarization-resolved IRRAS to investigate CO_2 adsorption on $CeO_2(110)$ single-crystal surfaces under well-controlled conditions. Measurements were carried out for fully oxidized substrates using both *s*- and *p*-polarized light, enabling a detailed analysis of adsorption geometries via transition dipole moment selection rules. The structural quality of the $CeO_2(110)$ surface was verified by surface-ligand infrared spectroscopy (SLIR) using CO as a probe molecule and the amount of residual vacancies was determined by XPS. The spectra are dominated by the characteristic CO stretching vibrations associated with $CeO_2(110)$, confirming the high structural purity of the surface. From the XPS data, the residual amount of Ce^{3+} ions in the surface planes was determined to amount to roughly 10%.

Beyond its catalytic relevance, this work may inform actinide-oxide surface chemistry. CeO_2 serves as a non-radioactive surrogate for PuO_2, and both oxides show similar facet-dependent CO_2 adsorption, with stronger interactions at the open {100}/{110} surfaces than at {111}. Our carbonate fingerprints on $CeO_2(110)$ may thus benchmark theoretical studies of CO_2 adsorption on PuO_2, relevant to nuclear-material storage and environmental surface chemistry. Note that a previous study for CO adsorption on $UO_2(111)$ yielded rather similar results to CO on $CeO_2(111)$.[14]

In the IRRAS data, in addition to physisorbed CO_2 species, we clearly identify the formation of carbonate species. A band at 1510 cm^{-1} can be unambiguously assigned to a monodentate carbonate, in perfect agreement with the structure proposed by Saniz et al.[10] This assignment is further supported by the presence of a corresponding band at 1280 cm^{-1}, also observed in the experiments. The pronounced polarization dependence of these vibrational features is in excellent agreement with the adsorption geometry predicted by theory. Notably, despite extensive theoretical efforts, no additional carbonate species were identified on the stoichiometric surface. Therefore, we tentatively attribute the additional bands observed at 1570 and 1610 cm^{-1} to carbonate species formed at defective regions of the surface, such as step edges or oxygen vacancies.

EXPERIMENTAL SECTION

The surface was characterized by CO adsorption at 82 K (see Figure S1). A strong band at 2170 cm^{-1} was observed, characteristic for the $CeO_2(110)$ surfaces.[15,16] A low-intensity band at 2154 cm^{-1} indicated a small (less than 10%) fraction of (111) facets, typical for $CeO_2(110)$ surfaces.[17]

In Figure 1 we show experimental IRRAS data recorded after exposure to 5 Langmuir (L) of CO_2 at a temperature of 125 K. We clearly observe a double-peaked feature at 2350 cm^{-1} in p-polarized light and a single peak in s-polarized light, which can be assigned to physisorbed, linear CO_2, similar to $CeO_2(111)$

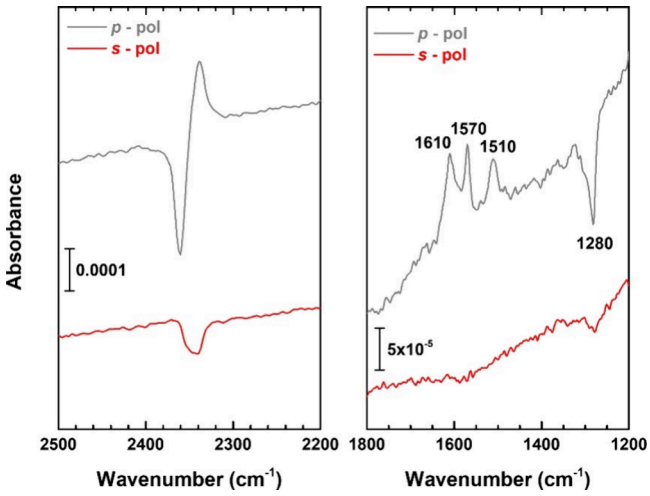


Figure 1. p- and s-polarized IRRA spectra of CO_2 at the fully oxidized $CeO_2(110)$ surface. The sample was exposed to 5 Langmuir of CO_2 at 125 K.

and other oxides such as Al_2O_3.[13] The splitting of the asymmetric stretch is a result of the so-called Berreman effect.[18] For a dielectric substrate, the tangential and surface-normal components of p-polarized light contribute to the IRRAS signal with opposite signs and slightly different frequencies. Consequently, the sign of an IRRAS band depends on the orientation of its transition dipole moment. This accounts for both the positive/negative Berreman-type feature of physisorbed CO_2 near 2350 cm^{-1} and the opposite phases of the carbonate stretching bands. For a more detailed discussion see refs 13 and 18. For the cd-b carbonate, DFT predicts distinctly different TDM orientations for the asymmetric and symmetric O−C−O stretching modes, consistent with their opposite signs in the p-polarized spectrum. At lower wavenumbers, we observe, in p-polarized light, positive peaks at 1510, 1570, and 1610 cm^{-1}, and a negative peak at 1280 cm^{-1}. For s-polarized light, only a band at 1280 cm^{-1} can be seen.

When annealing the substrate, we found that the bands related to the physisorbed species disappear at around 150 K, consistent with the theoretical binding energies of 0.3−0.5 eV with the theoretical value for the 0.3−0.5 eV binding energy eV reported for these species.[10]

In a second set of experiments, exposure to CO_2 was carried out at 150 K, above the desorption temperature of physisorbed CO_2. The results shown in Figure 2 reveal that now the peaks at 2350 cm^{-1} are absent, only the peaks at about 1510 (1513 exactly), 1570, and 1610 (1627 exactly) cm^{-1} as well as the negative peak at 1280 cm^{-1} are left. The intensity of these peaks did not change significantly relative to the adsorption at 125 K. As shown in Figure 3, the species at 1610 cm^{-1} exhibits a relatively low adsorption energy. As the temperature rises to 300 K, its peak intensity diminishes to the noise level, indicating nearly complete desorption at this temperature. By contrast, the species at 1510 cm^{-1} has the highest adsorption energy, as demonstrated by its slow decline in peak intensity with increasing temperature. The adsorption energy of the species at 1570 cm^{-1} lies between those of the other two species. Both the 1510 and 1570 species desorb completely upon heating to 400 K.

Previous studies have frequently assigned the absorption band at approximately 1610 cm^{-1} to adsorbed bicarbonate

https://doi.org/10.1021/acs.jpcc.6c06381
J. Phys. Chem. C XXXX, XXX, XXX−XXX

Downloaded from pubs.acs.org/jpccck/article-pdf/doi/10.1021/acs.jpcc.6c06381/6906427/acs.jpcc.6c06381.pdf by UNIV ULM user on 05 November 2026

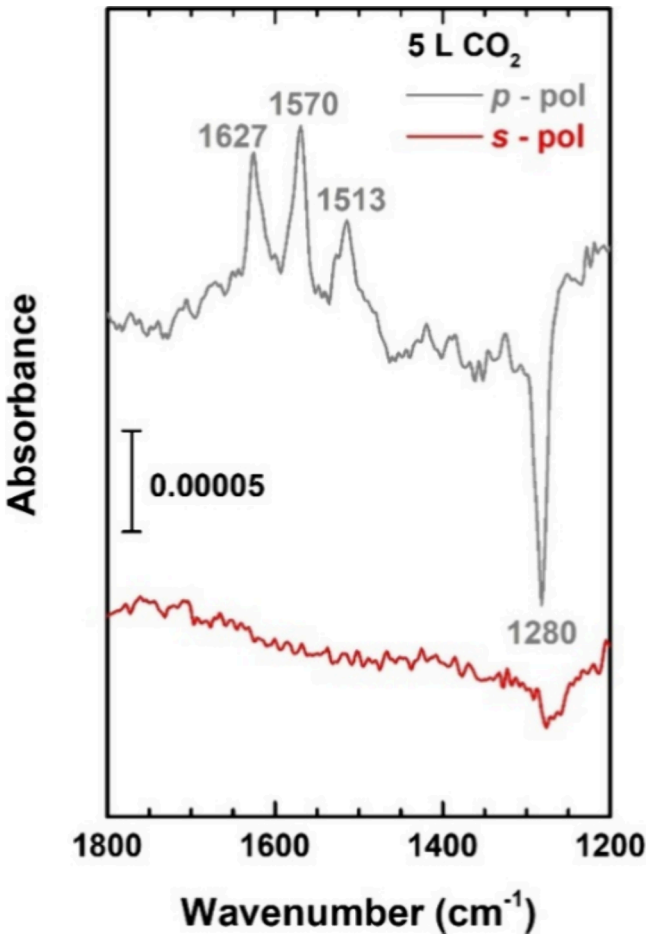


Figure 2. p- and s-polarized IRRA spectra of CO_2 at the fully oxidized $CeO_2(110)$ surface. The sample was exposed to 5 Langmuir of CO_2 at 150 K.

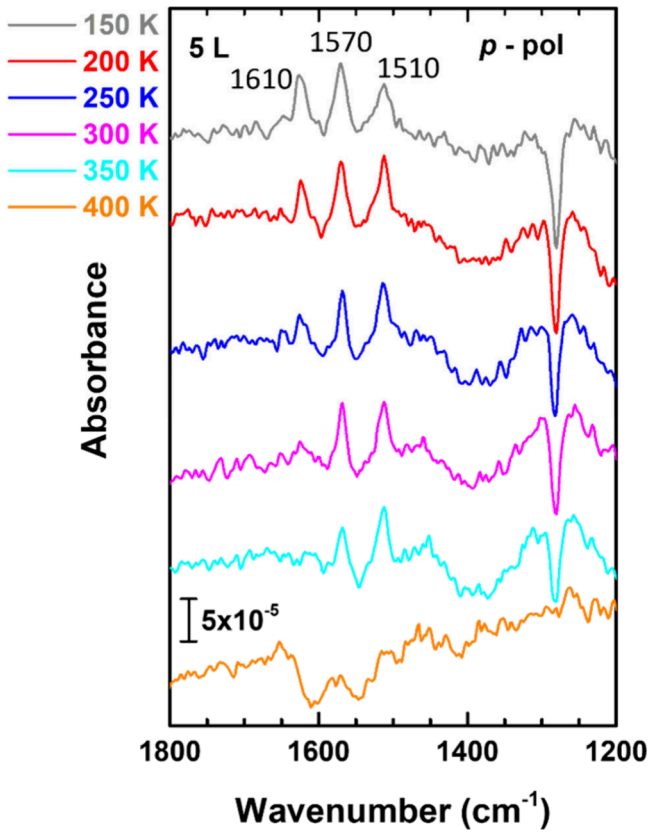


Figure 3. p-polarized IRRA spectra recorded directly after exposure to 5 L of CO_2 on the fully oxidized $CeO_2(110)$ surface (upper trace). The sample was gradually heated to indicated temperatures and spectra were recorded upon cooling back down to 150 K. The reported peak intensities reflect the species that survived the annealing process.

species (see, e.g., refs 12 and 19). However, this assignment appears unlikely for the present system. Both density functional theory calculations and experimental infrared studies of adsorbed bicarbonate consistently show that, in addition to the band near 1610 cm^{-1}, two further characteristic absorption bands should be observed at approximately 1400 and 1200 cm^{-1}. These three bands have been assigned to the ν_as(CO), ν_s(CO), and δ(COH) vibrational modes of surface bicarbonate species, respectively.[9,20] While our IRRAS data of CO_2 adsorbed on $CeO_2(110)$ exhibit a distinct band at 1610 cm^{-1}, no corresponding absorption features are detected in the 1400 or 1200 cm^{-1} regions. The absence of these two characteristic bicarbonate vibrations strongly argues against the assignment of the 1610 cm^{-1} band to a bicarbonate species. We therefore conclude that this feature must originate from a different adsorbed surface species, e.g., near an oxygen vacancy or a step edge.

THEORETICAL SECTION

In the previous section, six positive and negative features were identified in the experimental s- and p-polarized IRRAS data, each exhibiting distinct characteristics. In order to shed light on the underlying adsorption species we conducted a systematic search across the configurational space of CO_2 adsorption geometries on CeO_2 (110) within the framework of periodic density functional theory (DFT). A total of 1008 different initial geometries on the (1×1), the (1×2), and the (2×2) surfaces were relaxed to the nearest local minimum of the potential energy surface as described in the Supporting Information. We discarded 202 of these calculations since they did either not converge or resulted in unphysical/irrelevant configurations, e.g., positive adsorption energy or dissociation of CO_2 into CO and O. The remaining 806 configurations were closely examined and categorized. Eventually, a multitude of different physisorbed and a total of seven unique chemisorbed states could be identified. The following discussion focuses on the antisymmetric and symmetric stretching modes f_1 and f_2 of these configurations. Additionally, numerical values on the bending modes f_3 can be found in Table S2 in the Supporting Information and a list of all calculated vibrational frequencies is available as stated in the Data Availability Statement. All electronic structure calculations were carried out with the VASP[21−23] code employing the projector augmented wave method[24] and the functional form of the flavor of Perdew, Burke, and Ernzerhof,[22] including the Hubbard-U approach[25] and Grimme's D3 correction scheme.[26] A thorough discussion on the computational details can be found in the Supporting Information.

Physisorbed states are characterized by weak adsorption energies in the order of a few hundred meV and only minor changes of the adsorbate spatial and electronic structure compared to its isolated state. Table 1 lists the adsorption energies and vibrational frequencies of all unique physisorbed

Downloaded from pubs.acs.org/jpccck/article-pdf/doi/10.1021/acs.jpcc.6c06381/69066427/acs.jpcc.6c06381.pdf by UNIV ULM user on 05 November 2026

https://doi.org/10.1021/acs.jpcc.6c06381
J. Phys. Chem. C XXXX, XXX, XXX−XXX

Table 1. Adsorption Energy E_{ads} and IR Frequency f_1 of All Unique Physisorbed Species that Resulted from Our Screening Categorized with Respect to the Investigated Slab Sizes[a]

	(1 × 1)		(1 × 2)		(2 × 2)	
	E_{ads}	f_1	E_{ads}	f_1	E_{ads}	f_1
sp1	−0.28	2352	−0.27	2343	−0.28	2356
sp3 (hh_a)	−0.45	2359	−0.45	2353	−0.46	2363
sp4			−0.42	2332	−0.42	2313
sp4-cr	−0.44	2338	−0.41	2328	−0.41	2324
sp5 (dh_b)			−0.43	2340	−0.43	2339
sp6 (oo_b)			−0.43	2327	−0.43	2325
sp6-cr	−0.37	2338				
sp7			−0.12	2352	−0.12	2350
sv1			−0.12	2365	−0.12	2361
sv2 (ct_c)	−0.21	2401	−0.23	2387	−0.24	2382
sv2-cr	−0.30	2375				
sv3			−0.06	2359	−0.06	2352
sv4			−0.12	2363	−0.12	2356

[a] E_{ads} is given in eV and f_1 in cm^{-1}. The labels are given in accordance with Cheng et al.[27] and Saniz et al.[10].

states resulting from our screening for three different coverages. The states are labeled in accordance with the work of Cheng et al.[27] who described 11 different physisorbed states. Here, "sp" indicates that the molecule is aligned *parallel* to the surface whereas "sv" indicates *vertical* orientation. In addition to that we found a few states to be crooked compared to these configurations, which we indicate by the suffix "-cr". In a more recent work, Saniz et al.[10] reported only four physisorbed states, the labels of which are given in brackets, too.

Overall, for the (1 × 2) and the (2 × 2) surfaces we find the configurations described by Cheng et al. except the state "sp2" which is associated with a CO_2 molecule centered on a surface Ce atom. The (1 × 1) surface exhibits less states compared to the larger surfaces. The crooked state "sp4-cr" is found on all three surfaces whereas the states "sp6-cr" and "sv2-cr" are found on the (1 × 1) surface only. Hence, we find a multitude of different physisorbed configurations and do not agree with the claim of Saniz et al. that only four unique geometries exist. The adsorption energies we found differ significantly from the ones reported by Cheng et al. but agree qualitatively rather well with Saniz et al. The differences are to be attributed to the different functionals used. In particular, Cheng et al. did not consider dispersion interactions that may have deteriorated their results, as discussed in the Supporting Information.

The frequency f_1 reported in Table 1 corresponds to the asymmetric stretch vibration.[28] Other vibrations (reported in the SI) show intensities reduced by a factor of at least 5−10 in most cases compared to the asymmetric stretch vibration and are thus not expected to be visible in the experimental spectrum. The majority of the frequencies show numerical values of f_1 = 2340−2365 cm^{-1}, but also values as low as f_1 = 2313 cm^{-1} and as high as f_1 = 2400 cm^{-1} are found. These results indicate that the vibrational modes of the physisorbed states only slightly deviate from the vibrations of the isolated molecule which was calculated to 2365 cm^{-1} (cf. Supporting Information). In Figure 4, the geometry of four selected configurations on the (2 × 2) surface is displayed and the transition dipole moment (TDM) $\vec{\mu}$ is given as an example. As a general result for the case of physisorption we find the expected result that the transition dipole moment fully aligns with the orientation of the linear CO_2 molecule.

Chemisorption on the other hand is associated with much stronger adsorption energies which are typically accompanied by changes in the geometry and electronic structure of the adsorbed molecule. While several earlier theoretical studies did not find any chemisorbed state for CO_2 on the CeO_2(110) surface,[27,29−31] more recent works reported one chemisorbed state.[10,32,33] Our comprehensive search reported here resulted in a total of seven unique chemisorbed states for which the adsorption energies and two vibrational frequencies are listed in Table 2.

Within our data set, we found the carbon down b-species to exhibit the strongest binding energy. The calculated bond lengths and angles of this species (Figure 5a) agree very favorably with those of the chemisorbed species identified by Saniz and co-workers[10] (called ot_b in their study as indicated in Table 2), who characterized it as monodentate carbonate. The binding energies determined in our analysis, E_{ads} = −1.32 eV on the (1 × 2) and E_{ads} = −1.42 eV on the (2 × 2) surface, support the finding of Saniz et al. that the adsorption strength decreases with increasing coverage. The absolute binding energy values are somewhat below those reported in the Saniz work (a difference of 0.35 eV in the case of the (2 × 2) surface) but are in very good agreement with those of Symington et al.,[32] the difference being most likely due to the different treatment of dispersion interactions in the respective studies. We were not able to stabilize this species for the higher coverage using a smaller (1 × 1) surface unit cell (corresponding to unity coverage), the reason being the repulsion of the oxygen atoms of the two neighboring carbonates. The calculated asymmetric and symmetric stretch frequencies of the cd-b species amount to 1515 and 1254

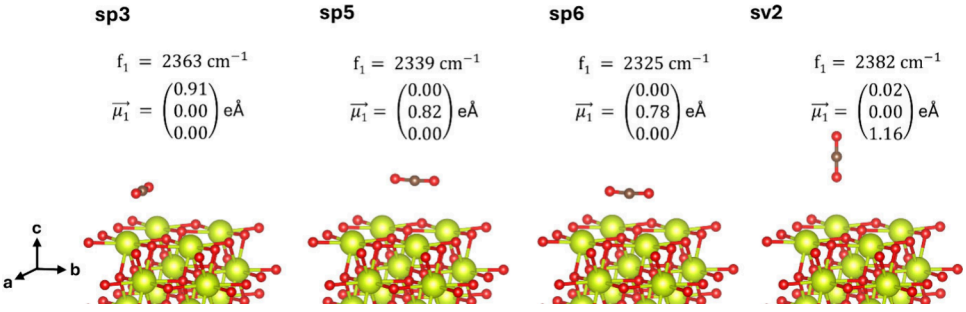


Figure 4. Adsorption configurations of four selected physisorbed states on the (2 × 2) surface including the respective antisymmetric stretch frequency f_1 and the TDM $\vec{\mu}_1$.

https://doi.org/10.1021/acs.jpcc.6c06381
J. Phys. Chem. C XXXX, XXX, XXX−XXX

Downloaded from pubs.acs.org/jpccck/article-pdf/doi/10.1021/acs.jpcc.6c06381/6906427/acs.jpcc.6c06381.pdf by UNIV ULM user on 05 November 2026

Table 2. Adsorption Energy E_{ads} and IR Frequencies of the Unique Chemisorbed Species on the Investigated Slab Sizes[a]

	(1 × 1)			(1 × 2)			(2 × 2)		
	E_{ads}	f_1	f_2	E_{ads}	f_1	f_2	E_{ads}	f_1	f_2
cd-a	−0.77	1487	1253	−0.90	1477	1231	−0.83	1502	1203
cd-b (ot_b)				−1.32	1517	1253	−1.42	1515	1254
fl-a				−0.92	1420	1258			
fl-b				−0.83	1405	1238	−0.53	1425	1223
so-a	−0.41	1716	1116						
so-b							−0.45	1174	1558
br-b							−0.71	1109	1613

[a] E_{ads} is given in eV and f_i in cm^{-1}. The first part of the naming abbreviates carbon down as "cd", flat as "fl", side-on as "so", and bridged as "br" whereas the letter indicates the orientation of the molecule.

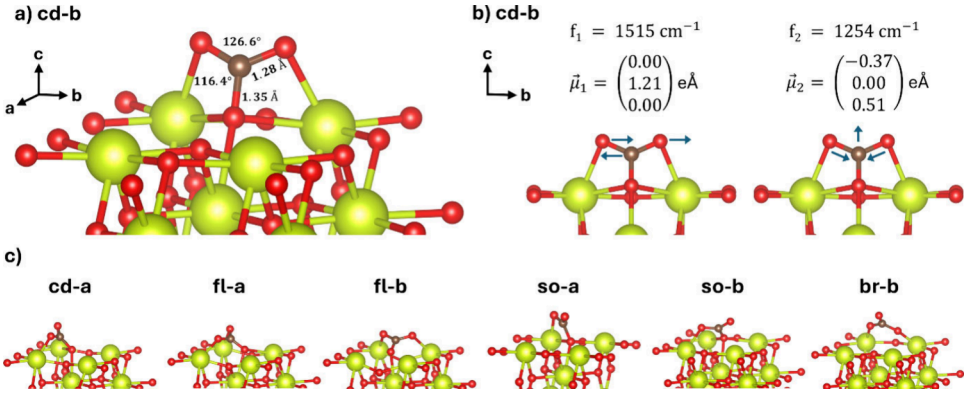


Figure 5. (a) Adsorption configuration cd-b including bond lengths and angles. (b) Antisymmetric and symmetric stretch modes, including vibrational frequencies and TDMs of the cd-b species. (c) Adsorption configurations of the other unique chemisorbed species.

cm^{-1}, respectively. The corresponding modes and TDMs are indicated in Figure 5b and are oriented parallel to the substrate for the former and tilted upward from the surface for the latter.

In addition to the cd-b species, six other adsorbate configurations were stabilized in our screening that had not been reported to date, all of them carbonate-like species (Table 2 and Figure 5c). Many of these species exhibit adsorption energies in the intermediate range from E_{ads} = −0.71 eV to E_{ads} = −0.92 eV, but there are weakly bound species with E_{ads} = −0.41 eV to E_{ads} = −0.53 eV as well. The configuration of species cd-a is geometrically similar to the cd-b species but rotated by 90° around the surface normal, now with the O−O axis oriented along the a-direction. Species cd-a is stabilized at all surface sizes studied here, exhibiting frequencies a little (10−50 cm^{-1}) below the ones of species cd-b. The configurations of species fl-a and fl-b resemble species cd-a and cd-b with the CO_3^{2-} plane being tilted slightly more toward the surface plane. In the case of fl-a the surface-O which takes part in the carbonate is slightly displaced whereas for fl-b the flat geometry is achieved by anchoring the carbonate to a different surface-O compared to the cd-b configuration. The frequencies of these species amount to f_1 = 1405−1425 cm^{-1} and f_2 = 1223−1258 cm^{-1}. The so-a/b species exhibit interestingly low adsorption energies of E_{ads} = −0.41/−0.45 eV, which are comparable to many physisorbed species. The TDMs of all unique chemisorbed species are provided in Figure S3 in the Supporting Information.

DISCUSSION

At first sight, it appears puzzling that after exposure of $CeO_2(110)$ to CO_2 at 125 K a coexistence of physisorbed and chemisorbed states with rather different binding energies is observed, in accordance with previous work using XPS and NEXAFS for the same system.[7] This observation effectively rules out that the adsorbate system is in thermodynamic equilibrium. Indeed, previous theoretical work has proposed that the distribution of adsorption states is governed by adsorption dynamics and energy dissipation pathways, leading to kinetic trapping in metastable configurations rather than thermodynamic equilibrium.

The situation becomes simpler when adsorption is carried out at 150 K. At this higher temperature, the physisorbed species is no longer stable, and only chemisorbed species are formed. At this higher temperature, the absolute as well as the relative intensities of the bands at 1510, 1570, and 1610 cm^{-1} remain unchanged.

Using our theoretical results, the vibrational band at 2350 cm^{-1} can be assigned to the multitude of physisorbed states, many of which are assumed to coexist as their adsorption energies are rather similar around $E_{ads} \approx -0.4$ eV. Additionally, the vibrations at 1510 and 1280 cm^{-1} can be assigned to the asymmetric and symmetric stretching vibrations of the most stable carbonate species cd-b. The difference between experimental and theoretical values for the symmetric stretch frequency f_2 amounts to just under 30 cm^{-1} which is well within the error observed in other theoretical studies using similar methods.[34] The computed frequencies of the remaining six less strongly bound chemisorbed species cannot be observed in the experimental spectrum, rendering their existence rather unlikely. We therefore speculate that these configurations are metastable and convert to the energetically more favorable cd-b configuration.

At present, we are unable to provide a precise assignment of the additional species at 1570 and 1610 cm^{-1}. As discussed in

Downloaded from pubs.acs.org/jpccck/article-pdf/doi/10.1021/acs.jpcc.6c06381/6906427/acs.jpcc.6c06381.pdf by UNIV ULM user on 05 November 2026

https://doi.org/10.1021/acs.jpcc.6c06381
J. Phys. Chem. C XXXX, XXX, XXX−XXX

the experimental part, the presence of bicarbonate species can be excluded. From the fact that the widths of these unassigned peaks are comparable to that of the carbonate species at 1510 cm^{-1}, we conclude that they correspond to two well-defined carbonate species with different binding geometries to the substrate. From the temperature dependence of the IRRAS data, we further conclude that the binding energy of the species at 1610 cm^{-1} is lower than that at 1570 cm^{-1}. Since no additional peaks are observed in the region where the symmetric carbonate stretch is expected (around 1280 cm^{-1}), we propose that the symmetric modes of these two unassigned species overlap with that of the carbonate species exhibiting the asymmetric vibration at 1510 cm^{-1}. Indeed, the spectra (see Figure 1) reveal a slight asymmetry in this region.

While a definitive assignment cannot be made in the absence of solid experimental or theoretical evidence, the most likely explanation is that the two unassigned bands arise from carbonate species bound to substrate sites with strongly relaxed O and Ce atom positions — for instance, in the vicinity of oxygen vacancies or at step edges. Such configurations were not captured in our computational screening of adsorbate geometries, which was restricted to the stoichiometric surface, and may therefore account for vibrational signatures that fall outside the range of the calculated reference frequencies. We consider this the most plausible interpretation currently available, though further targeted calculations — for example, explicitly modeling carbonate adsorption near defect sites — would be needed to confirm it.

CONCLUSIONS

In the present study, a combination of IRRAS experiments and DFT calculations was used to identify CO_2 adsorption species on CeO_2(110). The IRRAS experiments revealed five distinct vibrational bands of CO_2 on a well-defined CeO_2(110) single-crystal surface, three of which could be properly assigned to the theoretically obtained configurations after a comprehensive configurational search conducted with DFT: The band at 2350 cm^{-1} can be associated with the multitude of physisorbed species, while the bands at 1510 cm^{-1} and 1280 cm^{-1} can be related to the asymmetric and symmetric stretching vibrations of the monodentate carbonate cd-b. We speculate that the remaining two vibrational bands at 1570 and 1610 cm^{-1} correspond to adsorption species on surface defects or step edges, which were not included in the configurational search.

ASSOCIATED CONTENT

Data Availability Statement

Electronic structure calculations on all unique species that were obtained in this work (cf. Table S1), including the analysis of all vibrational frequencies and transition dipole moments, are made available under the Creative Commons Attribution license (CC BY 4.0) on the NOMAD repository (https://nomad-lab.eu) within the data set "CO2_on_Ceria_110", 10.17172/nomad.x3mh-qpzt.

Supporting Information

The Supporting Information is available free of charge at https://pubs.acs.org/doi/10.1021/acs.jpcc.6c06381.

Surface characterization of CeO_2(110) by IRRAS of adsorbed CO and by XPS (Figures S1 and S2); Experimental details; Adsorption energies, vibrational frequencies, and IR intensities of all unique adsorption configurations (Table S1); Geometries, vibrational frequencies, and transition dipole moments of all unique chemisorbed states (Figure S3); Computational details, including the generation of the input geometries for the configurational screening (Figure S4) and the benchmark of the computational settings (Table S2) (PDF)

AUTHOR INFORMATION

Corresponding Authors

Axel Groß − *Institute of Theoretical Chemistry, Ulm University, 89081 Ulm, Germany; Helmholtz Institute Ulm (HIU) for Electrochemical Energy Storage, 89081 Ulm, Germany;* orcid.org/0000-0003-4037-7331; Email: axel.gross@uni-ulm.de

Christof Wöll − *Institute of Functional Interfaces, IFG, Karlsruhe Institute of Technology, KIT, 76344 Eggenstein-Leopoldshafen, Germany; Ordos Laboratory, Ordos, Inner Mongolia 017010, China;* orcid.org/0000-0003-1078-3304; Email: christof.woell@kit.edu

Authors

Johannes Döhn − *Institute of Theoretical Chemistry, Ulm University, 89081 Ulm, Germany*

Chengwu Yang − *State Key Laboratory of Coal Conversion, Institute of Coal Chemistry, Chinese Academy of Sciences, Taiyuan 030001, China*

Complete contact information is available at: https://pubs.acs.org/10.1021/acs.jpcc.6c06381

Author Contributions

#These authors contributed equally to this work (J.D. and C.Y.).

Notes

The authors declare no competing financial interest.

ACKNOWLEDGMENTS

This work was funded by the National Key Research and Development Program of China (Grant Number 2022YFA1604100) and 2026 Science and Technology Support Project of Inner Mongolia Autonomous Region (Grant Number Ordoslab-kjzc-202604). This work also contributes to research carried out in the NETPEC2 project funded by the Bundesministerium für Forschung, Technologie und Raumfahrt (BMFTR), grant number 01LS2510B. Furthermore, J.D. gratefully acknowledges funding by Dr. Barbara-Mez-Starck Foundation and computer time provided by the state of Baden-Württemberg through bwHPC and the German Research Foundation (DFG) through grant no INST 40/575-1 FUGG (Justus 2 Cluster). C.Y. gratefully acknowledges the financial support of the Institute of Coal Chemistry, Chinese Academy of Sciences, State Key Laboratory of Coal Conversion and the Department of Human Resources and Social Security of Shanxi Province.

REFERENCES

(1) Ye, J.; Dimitratos, N.; Rossi, L. M.; Thonemann, N.; Beale, A. M.; Wojcieszak, R. Hydrogenation of CO_2 for Sustainable Fuel and Chemical Production. *Science* **2025**, *387* (6737), No. eadn9388.

(2) Sakakura, T.; Choi, J.-C.; Yasuda, H. Transformation of Carbon Dioxide. *Chem. Rev.* **2007**, *107* (6), 2365−2387.

(3) Sahoo, P. K.; Zhang, Y.; Das, S. CO_2 -Promoted Reactions: An Emerging Concept for the Synthesis of Fine Chemicals and Pharmaceuticals. *ACS Catal.* **2021**, *11* (6), 3414−3442.

Downloaded from pubs.acs.org/jpccck/article-pdf/doi/10.1021/acs.jpcc.6c06381/6906427/acs.jpcc.6c06381.pdf by UNIV ULM user on 05 November 2026

(4) May, M. M.; Rehfeld, K. Negative Emissions as the New Frontier of Photoelectrochemical CO_2 Reduction. *Adv. Energy Mater.* **2022**, *12* (21), 2103801.
(5) Caulfield, L.; Sauter, E.; Idriss, H.; Wang, Y.; Wöll, C. Bridging the Pressure and Materials Gap in Heterogeneous Catalysis: A Combined UHV, In Situ, and Operando Study Using Infrared Spectroscopy. *J. Phys. Chem. C* **2023**, *127* (29), 14023−14029.
(6) Buchholz, M.; Yu, X.; Yang, C.; Heißler, S.; Nefedov, A.; Wang, Y.; Wöll, C. IR-Spectroscopy of CO Adsorption on Mixed-Terminated ZnO Surfaces. *Surf. Sci.* **2016**, *652*, 247−252.
(7) Yang, C.; Bebensee, F.; Chen, J.; Yu, X.; Nefedov, A.; Wöll, C. Carbon Dioxide Adsorption on CeO_2 (110): An XPS and NEXAFS Study. *ChemPhysChem* **2017**, *18* (14), 1874−1880.
(8) Baumann, N.; Lan, J.; Iannuzzi, M. CO2 Adsorption on the Pristine and Reduced CeO2 (111) Surface: Geometries and Vibrational Spectra by First Principles Simulations. *J. Chem. Phys.* **2021**, *154* (9), 094702.
(9) Vayssilov, G. N.; Mihaylov, M.; Petkov, P. St.; Hadjiivanov, K. I.; Neyman, K. M. Reassignment of the Vibrational Spectra of Carbonates, Formates, and Related Surface Species on Ceria: A Combined Density Functional and Infrared Spectroscopy Investigation. *J. Phys. Chem. C* **2011**, *115* (47), 23435−23454.
(10) Saniz, R.; Li, S.; Lamoen, D.; Bogaerts, A.; Partoens, B. CO_2 Adsorption on Stoichiometric Ceria (110) Revisited. *J. Phys. Chem. C* **2025**, *129* (28), 12814−12826.
(11) Keller, F.; Döhn, J.; Groß, A.; Busch, M. Exploring the Mechanism of the Electrochemical Polymerization of CO_2 to Hard Carbon over CeO_2 (110). *J. Phys. Chem. C* **2024**, *128* (15), 6280−6293.
(12) Chen, S.; Cao, T.; Gao, Y.; Li, D.; Xiong, F.; Huang, W. Probing Surface Structures of CeO_2, TiO_2, and Cu_2 O Nanocrystals with CO and CO_2 Chemisorption. *J. Phys. Chem. C* **2016**, *120* (38), 21472−21485.
(13) Zerulla, B.; Krstić, M.; Chen, S.; Yu, Z.; Beutel, D.; Holzer, C.; Nyman, M.; Nefedov, A.; Wang, Y.; Mayerhöfer, T. G.; Wöll, C.; Rockstuhl, C. Polarization-Dependent Effects in Vibrational Absorption Spectra of 2D Finite-Size Adsorbate Islands on Dielectric Substrates. *Phys. Chem. Chem. Phys.* **2024**, *26* (18), 13683−13693.
(14) Idriss, H.; Barral, M. A.; Di Napoli, S. M.; Murgida, G. E.; Sauter, E.; Llois, A. M.; Ganduglia-Pirovano, M. V.; Vildosola, V. L.; Wöll, C. Exploring Molecule-Surface Interactions of Urania via IR Spectroscopy and Density Functional Theory. *Phys. Chem. Chem. Phys.* **2025**, *27* (5), 2405−2417.
(15) Lustemberg, P. G.; Yang, C.; Wang, Y.; Wöll, C.; Ganduglia-Pirovano, M. V. Vibrational Frequencies of CO Bound to All Three Low-Index Cerium Oxide Surfaces: A Consistent Theoretical Description of Vacancy-Induced Changes Using Density Functional Theory. *J. Chem. Phys.* **2023**, *159* (3), 034704.
(16) Lustemberg, P. G.; Plessow, P. N.; Wang, Y.; Yang, C.; Nefedov, A.; Studt, F.; Wöll, C.; Ganduglia-Pirovano, M. V. Vibrational Frequencies of Cerium-Oxide-Bound CO: A Challenge for Conventional DFT Methods. *Phys. Rev. Lett.* **2020**, *125* (25), 256101.
(17) Yang, C.; Yu, X.; Heißler, S.; Nefedov, A.; Colussi, S.; Llorca, J.; Trovarelli, A.; Wang, Y.; Wöll, C. Surface Faceting and Reconstruction of Ceria Nanoparticles. *Angew. Chem., Int. Ed.* **2017**, *56* (1), 375−379.
(18) Yang, C.; Wang, W.; Nefedov, A.; Wang, Y.; Mayerhöfer, T. G.; Wöll, C. Polarization-Dependent Vibrational Shifts on Dielectric Substrates. *Phys. Chem. Chem. Phys.* **2020**, *22* (30), 17129−17133.
(19) Panayotov, D.; Zdravkova, V.; Lagunov, O.; Andonova, S.; Spassova, I.; Nihtianova, D.; Atanasova, G.; Drenchev, N.; Ivanova, E.; Mihaylov, M.; Hadjiivanov, K. Capturing CO2 by Ceria and Ceria-Zirconia Nanomaterials of Different Origin. *Phys. Chem. Chem. Phys.* **2023**, *25* (26), 17154−17175.
(20) Baltrusaitis, J.; Grassian, V. H. Surface Reactions of Carbon Dioxide at the Adsorbed Water-Iron Oxide Interface. *J. Phys. Chem. B* **2005**, *109* (25), 12227−12230.
(21) Kresse, G.; Hafner, J. *Ab Initio* Molecular Dynamics for Liquid Metals. *Phys. Rev. B* **1993**, *47* (1), 558−561.
(22) Kresse, G.; Furthmüller, J. Efficiency of Ab-Initio Total Energy Calculations for Metals and Semiconductors Using a Plane-Wave Basis Set. *Comput. Mater. Sci.* **1996**, *6* (1), 15−50.
(23) Kresse, G.; Joubert, D. From Ultrasoft Pseudopotentials to the Projector Augmented-Wave Method. *Phys. Rev. B* **1999**, *59* (3), 1758−1775.
(24) Blöchl, P. E. Projector Augmented-Wave Method. *Phys. Rev. B* **1994**, *50* (24), 17953−17979.
(25) Dudarev, S. L.; Botton, G. A.; Savrasov, S. Y.; Humphreys, C. J.; Sutton, A. P. Electron-Energy-Loss Spectra and the Structural Stability of Nickel Oxide: An LSDA+U Study. *Phys. Rev. B* **1998**, *57* (3), 1505−1509.
(26) Grimme, S.; Antony, J.; Ehrlich, S.; Krieg, H. A Consistent and Accurate *Ab Initio* Parametrization of Density Functional Dispersion Correction (DFT-D) for the 94 Elements H-Pu. *J. Chem. Phys.* **2010**, *132* (15), 154104.
(27) Cheng, Z.; Sherman, B. J.; Lo, C. S. Carbon Dioxide Activation and Dissociation on Ceria (110): A Density Functional Theory Study. *J. Chem. Phys.* **2013**, *138* (1), 014702.
(28) Burghaus, U. Surface Chemistry of CO2 - Adsorption of Carbon Dioxide on Clean Surfaces at Ultrahigh Vacuum. *Prog. Surf. Sci.* **2014**, *89* (2), 161−217.
(29) Kumari, N.; Haider, M. A.; Agarwal, M.; Sinha, N.; Basu, S. Role of Reduced CeO_2 (110) Surface for CO_2 Reduction to CO and Methanol. *J. Phys. Chem. C* **2016**, *120* (30), 16626−16635.
(30) Kumari, N.; Sinha, N.; Haider, M. A.; Basu, S. CO 2 Reduction to Methanol on CeO 2 (110) Surface: A Density Functional Theory Study. *Electrochim. Acta* **2015**, *177*, 21−29.
(31) Marciniak, A. A.; Henrique, F. J. F. S.; De Lima, A. F. F.; Alves, O. C.; Moreira, C. R.; Appel, L. G.; Mota, C. J. A. What Are the Preferred CeO2 Exposed Planes for the Synthesis of Dimethyl Carbonate? Answers from Theory and Experiments. *Mol. Catal.* **2020**, *493*, 111053.
(32) Symington, A. R.; Harker, R. M.; Storr, M. T.; Molinari, M.; Parker, S. C. Thermodynamic Evolution of Cerium Oxide Nanoparticle Morphology Using Carbon Dioxide. *J. Phys. Chem. C* **2020**, *124* (42), 23210−23220.
(33) Zhu, D.; Liu, H.; Huang, Y.; Luo, X.; Mao, Y.; Liang, Z. Study of Direct Synthesis of DMC from CO_2 and Methanol on CeO_2: Theoretical Calculation and Experiment. *Ind. Eng. Chem. Res.* **2022**, *61* (30), 10804−10817.
(34) Miyazaki, R.; Faraji, S.; Levchenko, S. V.; Foppa, L.; Scheffler, M. Vibrational Frequencies Utilized for the Assessment of Exchange-Correlation Functionals in the Description of Metal-Adsorbate Systems: C_2 H_2 and C_2 H_4 on Transition-Metal Surfaces. *Catal. Sci. Technol.* **2024**, *14* (23), 6924−6933.

Downloaded from pubs.acs.org/jpccck/article-pdf/doi/10.1021/acs.jpcc.6c06381/6906427/acs.jpcc.6c06381.pdf by UNIV ULM user on 05 November 2026